

Orientation Distribution of Cellulose Crystallites in Woody Plants. Part I. Pole-Figures and Orientation Functions of Cellulose Crystallites in Opposite Wood of *Pinus densiflora*.

Fumio TANAKA*, Tetsuto TAKAKI**, Keizo OKAMURA***
and Tetsuo KOSHIJIMA*

Abstract—Pole-Figures and orientation functions of cellulose in *Pinus densiflora* were measured. By semi-quantitatively evaluating the crystal data a valid model for cellulose crystallite orientation was proposed, which gives a plausible answer to explain the mechanical properties of the opposite wood of *Pinus densiflora*.

Introduction

Since the amount of wood replenished each year is limited, wood has to be wisely utilized. For this purpose one has to know all the aspects of wood from both physical and chemical point of view. In this series of studies, we concern factors which are especially related to the mechanical properties of wood. Among them the orientation distribution of cellulose crystallites in wood is important. In this paper, orientation distribution of cellulose crystallites in opposite wood of *Pinus densiflora* is reported.

On the crystallite orientations quite a few papers have been so far reported^{1,2,3}), but the distribution of the crystallite orientation was never reported due to the lack of three dimensional crystallite orientation distribution of specimen. Using a pole-figure device attached to X-ray equipment three dimensional description of crystallite orientation distributions^{4,5}) were studied. Semi-quantitative evaluations of the crystallite orientation distribution in opposite wood of *Pinus densiflora* are discussed.

Experimentals

In general, a great number of pole-figure X-ray data are required to determine the crystallite orientation distribution⁶). In this paper, however, only two crystallographic

* Division of Wood Chemistry

** Faculty of Agriculture, Kinki University, Higashi-Osaka, Osaka, 577 Japan

*** Faculty of Agriculture, Kyoto University, Kyoto, 606 Japan

planes, (400) and (004) planes*, on the equatorial line with $d=3.85\text{\AA}$ and 2.59\AA , are measured because of the lattice symmetry of the cellulose crystal.

Specimen

The blocks of opposite wood of *Pinus densiflora* obtained from Kamigamo Experimental Forest, University Forest, Kyoto University was used for this investigation. A Cartesian coordinate was set for sample space. In this coordinate we set the sample as such the normal (N), the transverse (T) and the longitudinal (L) directions respectively coincide with the radial, the tangential and the longitudinal directions in wood.

Description of Apparatus

A Rigaku Denki Roter Flex RU-100 diffractometer was used with pole-figure attachment.

The Procedure of Pole-Figure Measurement

Two techniques were used for pole-figure measurement : transmission and reflection technique⁷⁾. In the transmission technique shown in Figure 1, the Z-axis coincides with the goniometer axis, and X-Y plane includes the incident and diffracted X-ray beams and center of the specimen. When $\alpha=0^\circ$, the plane of the specimen is parallel to the plane Y-Z, and the L-axis of the specimen coincides with the Z-axis of the coordinate system fixed on the goniometer. With $\alpha=0^\circ$, the poles of the diffracting planes, which are coincident with Y-axis, lie in the plane of the specimen, and rotation of the specimen about its normal which coincides with N-axis (β -rotation), has the effect of scanning the periphery of the pole-figure (the 0° latitude circle). For the circumferences at higher latitudes the intensity can be scanned by rotating the specimen about the Z-axis by the desired α value and then rotating the specimen about its normal axis

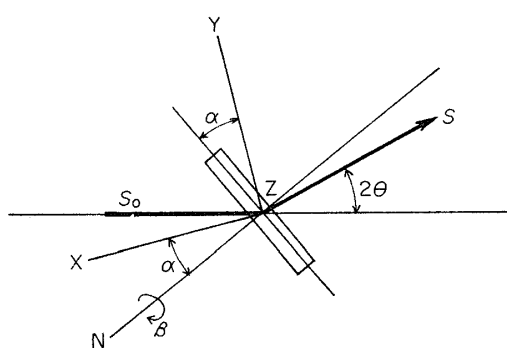


Fig. 1. Geometry for transmission technique.

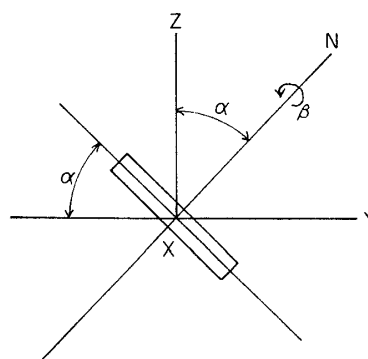


Fig. 2. Geometry for reflection technique.

* The monoclinic unit cell dimensions with $a=15.7\text{\AA}$, $b=16.42\text{\AA}$, $c(\text{fiber axis})=10.34\text{\AA}$, $\gamma=96.8^\circ$ was used throughout indexing diffraction planes⁷⁾. In keeping with the nomenclature presently in use in polymer crystallography, and c is designated the fiber axis and monoclinic angle (γ) is obtuse, (400) and (004) planes in the present unit cell correspond to (002) and (040) planes in terms of Meyer-Misch unit cell⁸⁾ with $a=8.14\text{\AA}$, $b(\text{fiber axis})=10.34\text{\AA}$, $c=7.85\text{\AA}$ and $\beta=83.4^\circ$.

(β -rotation). There are several techniques in reflection methods. In this experiment, the technique described by Schulz was used⁹⁾. The outline of this reflection technique is shown in Figure 2. The specimen is rotated around the X-axis by angle α and around N-axis by angle β . When $\alpha=0^\circ$, the plane of the specimen lies in the equatorial X-Y plane and the N-axis coincides with the Z-axis. With $\beta=0^\circ$, the L-axis is set parallel to the X-axis for this $\alpha=0^\circ$ geometry. The outer region of the pole (from $\alpha=0^\circ$ to $\alpha=60^\circ$) was covered by the transmission technique, and the inner region (from $\alpha=40^\circ$ to $\alpha=90^\circ$) was measured by reflection technique. The overlapped region $\alpha=40^\circ$ to $\alpha=60^\circ$ were used to match the intensity data so that transmission and reflection intensities can be treated on the same basis.

Intensity Correction

Since the X-ray path length in the specimen and accordingly the irradiated volume of the specimen vary with the specimen orientation with respect to incident and diffracted beam, absorption and volume corrections as well as the background scattering correction must be applied. Since the polarization and Lorentz factors depend only on the Bragg angle θ , these two factors need not be considered because of the averaged representation of the biaxial orientation for each crystallographic plane.

The background correction was experimentally done by the same procedure for pole-figure measurement without attaching sample in this case. The absorption and volume correction factors, R, for transmission technique are obtained by the following equation⁴⁾:

$$R = \frac{I(\alpha=\alpha)}{I(\alpha=0)} = \frac{\cos(\theta) [\exp\{-\mu t/\cos(\theta-\alpha)\} - \exp\{-\mu t/\cos(\theta+\alpha)\}]}{\mu t \exp\{-\mu t/\cos(\theta)\} \{ \cos(\theta-\alpha)/\cos(\theta+\alpha) - 1 \}}$$

where μ is a linear absorption coefficient, t , specimen thickness, θ , Bragg angle and α , the angle shown in Figure 1. These absorption and volume correction factors were also experimentally evaluated for the reflection technique using cellulose powder.

Results and Discussion

Tables I and II show the normalized orientation distributions for (400) and (004) planes. Figure 3 shows the pole-figure diagrams of the (400) and (004) planes of the cellulose crystallites in opposite wood of *Pinus densiflora*. These are on the basis of the stereographic projection along the normal direction of the sample surface. The Alabic numerals in these figures represent the qualitative distribution density ratio.

In the diagram of (400) planes, the pole density distribution shows that the (400) plane normals are almost perpendicular to the longitudinal direction, and have cylindrical symmetry around this direction. In the (004) planes, the maximum point of the pole density distribution are on the longitudinal direction, which means that cellulose chains in the opposite wood are along the longitudinal direction of the sample. The

Table I. Normalized orientation distribution for (400) planes.

$\alpha \backslash \beta$	0	10	20	30	40	50	60	70	80	90
90	3.14	3.14	3.14	3.14	3.14	3.14	3.14	3.14	3.14	3.14
80	1.26	1.43	1.41	1.56	1.69	1.89	2.22	2.74	3.09	3.92
70	0.63	0.64	0.73	0.77	0.88	1.06	1.42	1.92	2.64	3.62
60	0.40	0.50	0.45	0.50	0.65	0.70	0.96	1.39	2.28	3.30
50	0.39	0.30	0.34	0.30	0.38	0.46	0.62	1.06	1.98	2.83
40	0.35	0.40	0.42	0.31	0.28	0.38	0.48	0.88	1.55	2.48
30	0.35	0.37	0.41	0.33	0.23	0.21	0.26	0.52	1.06	1.98
20	0.13	0.15	0.19	0.27	0.25	0.16	0.21	0.36	0.79	1.57
10	0.15	0.15	0.12	0.23	0.24	0.15	0.17	0.32	0.72	1.53
0	0.13	0.12	0.11	0.20	0.25	0.18	0.17	0.31	0.70	1.69

Table II. Normalized orientation distribution for (004) planes.

$\alpha \backslash \beta$	0	10	20	30	40	50	60	70	80	90
90	0.13	0.13	0.13	0.13	0.13	0.13	0.13	0.13	0.13	0.13
80	0.62	0.68	0.62	0.71	0.73	0.51	0.62	0.48	0.63	0.72
70	0.70	0.64	0.70	0.40	0.67	0.56	0.48	0.59	0.59	0.75
60	0.32	0.32	0.25	0.13	0.30	0.40	0.60	0.40	0.50	0.54
50	0.70	0.41	0.36	0.36	0.24	0.16	0.40	0.56	0.24	0.32
40	0.72	0.83	0.72	0.72	0.46	0.41	0.46	0.36	0.72	0.57
30	0.41	0.63	0.49	0.63	0.47	0.20	0.22	0.25	0.31	0.33
20	1.18	1.02	0.19	0.28	0.46	0.21	0.16	0.21	0.27	0.27
10	5.02	3.85	0.66	0.30	0.39	0.20	0.15	0.18	0.23	0.27
0	8.52	6.18	1.90	0.68	0.39	0.28	0.13	0.18	0.31	0.25

two pole-figure diagrams express that cellulose crystallites in opposite wood have cylindrical symmetry orientation distribution along the longitudinal direction.

Table III shows the three dimensional orientation functions of (400) and (004) planes of the opposite wood. Figure 4 shows the degree of biaxial orientation in terms of three orientation functions¹⁰⁾. The (400) planes mapped on the point represented in (a) indicate that the (400) planes of cellulose crystallites in the opposite wood have biaxial orientation and are nearly perpendicular to the longitudinal direction. The deviation of the point from the line N-T and the bisector of the angle between N-L and L-T represents the degree of orientation of the (400) planes. The (004) planes mapped on the point represented in (b) indicate that the (004) planes of cellulose crystallites are directed along the longitudinal direction, and the deviation of the point from the vertex L.D. represents the degree of orientation. It is clearly understood that the degree of orientation is excellent.

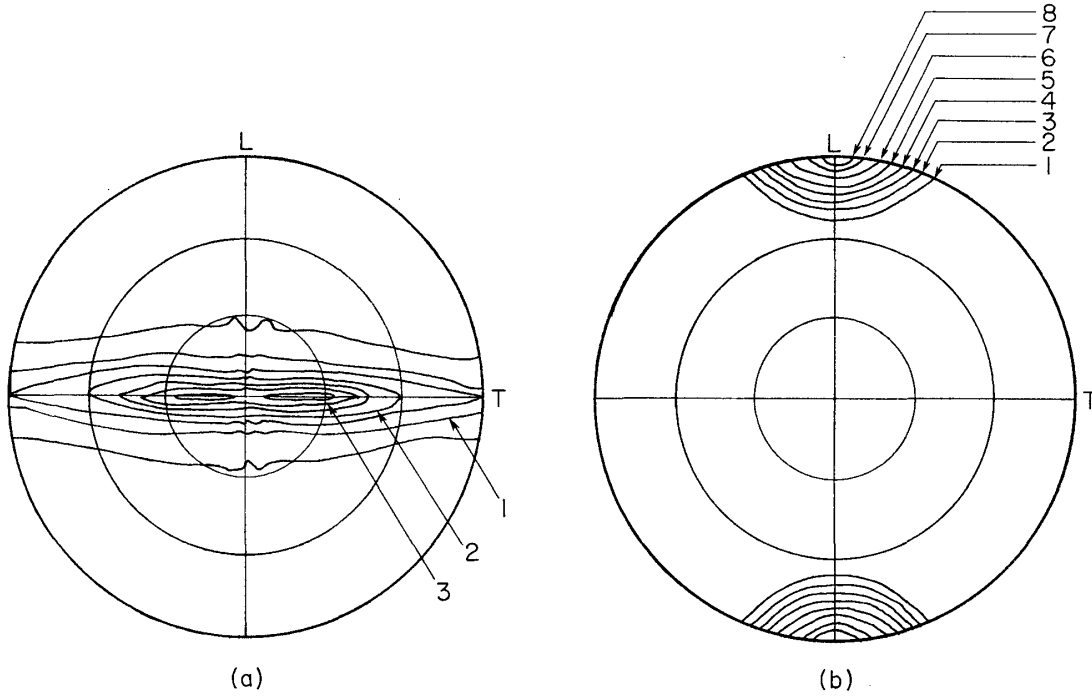


Fig. 3. Pole-Figure diagrams for (400) and (004) planes.
 (a): (400) planes and (b): (004) planes.

Table III. The orientation functions of (400) and (004) planes for each reference axes.

planes	reference axes		
	N. D.	T. D.	L. D.
(400)	0. 5107	0. 3621	0. 1114
(004)	0. 2537	0. 2045	0. 5684

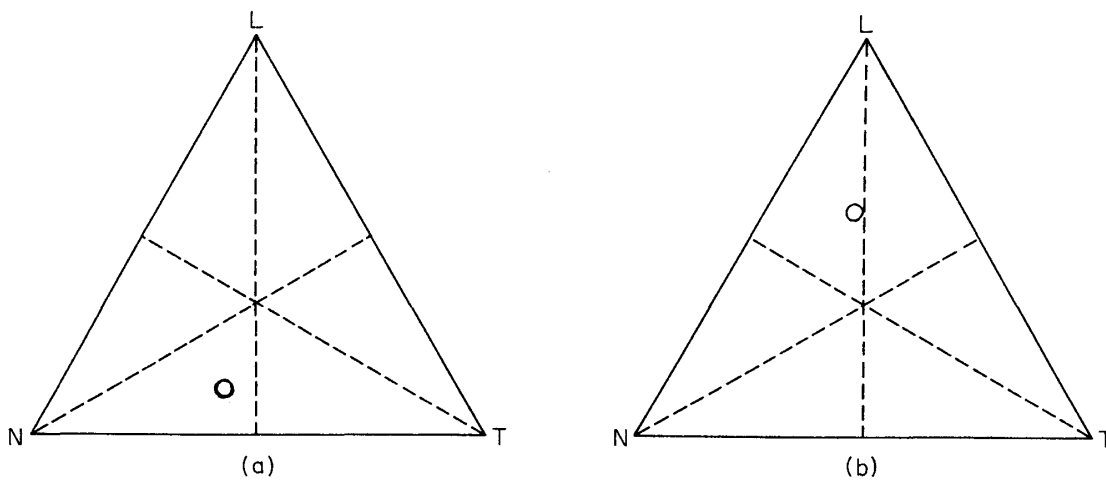


Fig. 4. Equilateral triangle diagrams representing the degree of biaxial orientation of cellulose crystallites in opposite wood of *Pinus densiflora* in terms of three orientation functions.
 (a): (400) planes and, (b): (004) planes.

Acknowledgement

We are greatly indebted to Kamigamo Experimental Forest, Kyoto University, for supplying the *Pinus densiflora* samples, and Mr. Takeshi Katsuyama, Wood Research Institute, Kyoto University, for preparation of the block samples of *Pinus densiflora*. We are indebted to the Data Processing Center, Kyoto University, for the use of FACOM M190.

References

- 1) H. Harada *et al.*; Bulletin Govt. Forest Sta., No. 104 (1958).
- 2) A. B. Wardrop; Holzforshung, **8**, 12 (1954).
- 3) R. D. Preston; "Molecular Architecture of Plant Cell Walls", Chapman & Hall, Ltd., London (1952).
- 4) B. D. Cullity; "Elements of X-Ray Diffraction", Addison-Wesley, Reading, Mass. (1956).
- 5) L. E. Alexander; "X-Ray Diffraction Methods in Polymer Science", John Wiley & Sons, Inc., New York (1969).
- 6) Z. W. Wilchinsky; J. Appl. Phys., **31**, 1969 (1960).
- 7) F. Tanaka and K. Okamura; J. Polym. Sci., Polymer Physics Edition, **15**, 897 (1977).
- 8) K. H. Meyer and L. Misch; Helv. Chim. Acta, **20**, 232 (1937).
- 9) L. C. Schulz; J. Appl. Phys., **20**, 1030 (1949).
- 10) C. R. Desper and R. S. Stein; J. Appl. Phys., **37**, 3990 (1966).